



HAL
open science

Potential energy surfaces without unphysical discontinuities: the Coulomb-hole plus screened exchange approach

Arjan Berger, Pierre-Francois Loos, Pina Romaniello

► To cite this version:

Arjan Berger, Pierre-Francois Loos, Pina Romaniello. Potential energy surfaces without unphysical discontinuities: the Coulomb-hole plus screened exchange approach. *Journal of Chemical Theory and Computation*, 2021, 17 (1), pp.191-200. 10.1021/acs.jctc.0c00896 . hal-02928385

HAL Id: hal-02928385

<https://hal.science/hal-02928385>

Submitted on 3 Sep 2020

HAL is a multi-disciplinary open access archive for the deposit and dissemination of scientific research documents, whether they are published or not. The documents may come from teaching and research institutions in France or abroad, or from public or private research centers.

L'archive ouverte pluridisciplinaire **HAL**, est destinée au dépôt et à la diffusion de documents scientifiques de niveau recherche, publiés ou non, émanant des établissements d'enseignement et de recherche français ou étrangers, des laboratoires publics ou privés.

Potential energy surfaces without unphysical discontinuities: the Coulomb-hole plus screened exchange approach

J. Arjan Berger,^{*,†,¶} Pierre-François Loos,[†] and Pina Romaniello^{‡,¶}

[†]*Laboratoire de Chimie et Physique Quantiques, Université de Toulouse, CNRS, UPS, France*

[‡]*Laboratoire de Physique Théorique, Université de Toulouse, CNRS, UPS, France*

[¶]*European Theoretical Spectroscopy Facility (ETSF)*

E-mail: arjan.berger@irsamc.ups-tlse.fr

Abstract

In this work we show the advantages of using the Coulomb-hole plus screened-exchange (COHSEX) approach in the calculation of potential energy surfaces. In particular, we demonstrate that, unlike perturbative GW and partial self-consistent GW approaches, such as eigenvalue-self-consistent GW and quasi-particle self-consistent GW , the COHSEX approach yields smooth potential energy surfaces without irregularities and discontinuities. Moreover, we show that the ground-state potential energy surfaces (PES) obtained from the Bethe-Salpeter equation, within the adiabatic connection fluctuation dissipation theorem, built with quasi-particle energies obtained from perturbative COHSEX on top of Hartree-Fock (BSE@COHSEX@HF) yield very accurate results for diatomic molecules close to their equilibrium distance. When self-consistent COHSEX quasi-particle energies and orbitals are used to build the BSE equation the results become independent of the starting point. We show that self-consistency worsens the total energies but improves the equilibrium distances with respect to BSE@COHSEX@HF. This is mainly due to changes in the screening inside the BSE.

1 Introduction

In the last decade the GW method¹⁻⁴ has become a standard tool in the quantum-chemistry tool box. It has proved to be a powerful approach for the calculation of ionization energies, electron affinities, fundamental gaps, etc. However, due to the complexity of the GW self-energy which is non-Hermitian and frequency dependent, a fully self-consistent approach is nontrivial.⁵⁻¹³ As a consequence, several approximate GW schemes have been devised. The most popular approaches are perturbative GW , also known as G_0W_0 ,¹⁴⁻¹⁹ eigenvalue self-consistent GW (ev GW)²⁰⁻²³ and quasi-particle self-consistent GW (qs GW).²⁴⁻²⁸ Within G_0W_0 , the GW self-energy is treated as a perturbation with respect to a zeroth-order Hamiltonian with a simpler self-energy, such as Hartree-Fock (HF), or a different Hamiltonian altogether, such as a Kohn-Sham Hamiltonian. The main drawback of G_0W_0 is its dependence on the choice of the starting point, i.e., the zeroth-order Hamiltonian.^{7,22,27-30} Within ev GW the dependence on the starting point is reduced by updating the eigenvalues in a self-consistent field procedure. However, the orbitals remain those of the zeroth-order Hamiltonian. Finally, within qs GW , the GW self-energy is approximated in such a way that it is both Hermitian and frequency independent. This allows for a simple self-consistent procedure for both eigenvalues and orbitals eliminating the influence of the starting point.

Although it is known that GW has some shortcomings, they have, until recently, mainly appeared in the strongly correlated regime.³¹⁻³⁹ However, in two recent articles,^{40,41} we uncovered an important shortcoming of the G_0W_0 , ev GW and qs GW approaches that appears in the weakly correlated regime. All three approaches suffer from unphysical irregularities and even discontinuities (ev GW and qs GW) in important physical quantities such as quasi-particle (QP) energies, neutral excitation energies, and correlation energies. We showed that the problem could be traced back to the existence of multiple close-lying solutions when the QP energy is close to a pole of the self-energy.^{18,40,41} When the solution switches from one branch to another one it yields an irregularity or discontinuity in the physical observable. The problem is more severe in ev GW and qs GW because, due to the self-consistency procedure, an irregularity in one QP energy is transferred to all QP energies through the self-consistent procedure.

This problem was again observed in the potential energy surfaces (PES) of diatomic molecules.⁴² Accurate results were obtained for the ground-state total energies from the adiabatic-connection fluctuation-dissipation theorem (ACFDT)^{43–53} applied to the Bethe-Salpeter equation (BSE) formalism.^{54–57} However, since the BSE calculations were performed on top of a G_0W_0 calculation, irregularities appeared in the energy curves due to the problem discussed above. As can be anticipated from our discussion above, switching to $evGW$ or $qsGW$ will not solve the problem. Below we will also explicitly show that discontinuities indeed appear in the PES when $evGW$ or $qsGW$ orbitals and energies are used to calculate the total energy. In view of the above, it is desirable to find an alternative approach to G_0W_0 , $evGW$ and $qsGW$ that does not suffer from this drawback and yields accurate total energies at an affordable computational cost.

In this work we will consider the Coulomb-hole plus screened-exchange (COHSEX) self-energy, which was proposed a long time ago by Hedin,^{1,20,58} both perturbatively, namely on top of HF, and self-consistently (scCOHSEX).⁵⁹ Although the physics inside the COHSEX self-energy is very similar to that included in the GW self-energy, unlike the GW self-energy, it is Hermitian and frequency independent. As a consequence, COHSEX calculations can be done self-consistently using standard numerical techniques (i.e., by simple diagonalization of a Fock-like operator). A self-consistent COHSEX calculation can also be used as starting point for a G_0W_0 or $evGW$ calculation.^{59–65} Such an approach generally yields accurate energy gaps but this would of course suffer from the same irregularities and discontinuities mentioned above. Thanks to its numerical efficiency COHSEX can be used to perform calculations on large systems.^{66,67} Finally, we note that improvements of the COHSEX method have been proposed.⁶⁸

The main goal of this work is twofold. We want to show that: (i) physical observables, and in particular PES, obtained within the COHSEX approach do not suffer from irregularities and discontinuities, and (ii) the PES and equilibrium geometries obtained from the BSE using perturbative COHSEX quasi-particle energies (i.e., BSE@COHSEX@HF) are comparable in accuracy to those obtained within BSE@ G_0W_0 . We illustrate both points by calculating the PES and equilibrium distances (R_{eq}) of several diatomic molecules. Furthermore we want to demonstrate that: (iii)

although the COHSEX and G_0W_0 energy gaps are quite different, the influence of this difference on the PES and equilibrium distances is small, and (iv) for the diatomic molecules studied here, perturbative COHSEX, i.e., BSE@COHSEX@HF, yields PES that are in better agreement with the reference values than self-consistent COHSEX, i.e., BSE@scCOHSEX. Instead, the values of R_{eq} obtained within BSE@scCOHSEX are slightly improved with respect to BSE@COHSEX@HF when compared to the reference data.

The paper is organized as follows. In section 2 we describe the theory behind the COHSEX approach and we also briefly discuss the theory of G_0W_0 and partially self-consistent GW methods. We report and discuss our results in section 3. Finally, in section 4 we draw the conclusions from our work.

2 Theory

The key variable within many-body perturbation theory is the one-body Green's function G . In the absence of time-dependent fields and at zero temperature, it is defined as

$$G(\mathbf{r}, \mathbf{r}', \tau) = -i\Theta(\tau) \langle \Psi_0^N | \hat{\psi}(\mathbf{r}) e^{-i(\hat{H}^N - E_0^N)\tau} \hat{\psi}^\dagger(\mathbf{r}') | \Psi_0^N \rangle + i\Theta(-\tau) \langle \Psi_0^N | \hat{\psi}^\dagger(\mathbf{r}') e^{i(\hat{H}^N - E_0^N)\tau} \hat{\psi}(\mathbf{r}) | \Psi_0^N \rangle, \quad (1)$$

where \hat{H}^N is the Hamiltonian of the N -electron system, Ψ_0^N is its ground-state wave function, E_0^N is the ground-state energy, Θ is the Heaviside step function, while $\hat{\psi}^\dagger$ and $\hat{\psi}$ are creation and annihilation operators, respectively. In practice the one-body Green's function can be obtained from the solution of the following Dyson equation,

$$G(\mathbf{r}, \mathbf{r}', \tau) = G_{\text{HF}}(\mathbf{r}, \mathbf{r}', \tau) + \iint d\mathbf{r}_1 d\mathbf{r}_2 G_{\text{HF}}(\mathbf{r}, \mathbf{r}_1, \tau) \Sigma_c(\mathbf{r}_1, \mathbf{r}_2, \tau) G(\mathbf{r}_2, \mathbf{r}', \tau), \quad (2)$$

where G_{HF} is the one-body Green's function within the HF approximation and Σ_c is the correlation part of the self-energy which has to be approximated in practical calculations.

2.1 The COHSEX self-energy

In this section we discuss the COHSEX self-energy, and, in particular, its correlation part. We will compare it to the GW self-energy since the two self-energies are similar. The correlation part of the GW and COHSEX self-energies are given by

$$\Sigma_c^{\text{GW}}(\mathbf{r}, \mathbf{r}', \tau) = iG(\mathbf{r}, \mathbf{r}', \tau)W_p(\mathbf{r}, \mathbf{r}', \tau + \eta), \quad (3a)$$

$$\Sigma_c^{\text{COHSEX}}(\mathbf{r}, \mathbf{r}', \tau) = iG(\mathbf{r}, \mathbf{r}', \tau)W_p(\mathbf{r}, \mathbf{r}', \omega = 0)[\delta(\tau + \eta) + \delta(\tau - \eta)]/2, \quad (3b)$$

where $W_p = W - v$, is the difference between the screened Coulomb interaction W and the bare Coulomb interaction v , δ is the Dirac delta function, and η is a positive infinitesimal that ensures the correct time ordering. The main difference between the two approximations is that the GW self-energy contains a dynamical (i.e., frequency dependent) W_p while the COHSEX self-energy has a static (i.e., frequency independent) W_p . A Fourier transformation of Eqs. (3a) and (3b) yields the following two expressions

$$\Sigma_c^{\text{GW}}(\mathbf{r}, \mathbf{r}', \omega) = \frac{i}{2\pi} \int d\omega' e^{i\eta\omega'} G(\mathbf{r}, \mathbf{r}', \omega + \omega') W_p(\mathbf{r}, \mathbf{r}', \omega'), \quad (4a)$$

$$\begin{aligned} \Sigma_c^{\text{COHSEX}}(\mathbf{r}, \mathbf{r}') &= \frac{i}{2} [G(\mathbf{r}, \mathbf{r}', -\eta) + G(\mathbf{r}, \mathbf{r}', \eta)] W_p(\mathbf{r}, \mathbf{r}', \omega = 0) \\ &= \frac{1}{2} \langle \Psi_0^N | \hat{\psi}(\mathbf{r}) \hat{\psi}^\dagger(\mathbf{r}') - \hat{\psi}^\dagger(\mathbf{r}') \hat{\psi}(\mathbf{r}) | \Psi_0^N \rangle W_p(\mathbf{r}, \mathbf{r}', \omega = 0), \end{aligned} \quad (4b)$$

and clearly shows that the COHSEX self-energy is static. We note that to better understand the screened exchange (SEX) and the Coulomb hole (COH) parts of the COHSEX self-energy it is useful to rewrite Eq. (4b) according to

$$\begin{aligned} \Sigma_c^{\text{COHSEX}}(\mathbf{r}, \mathbf{r}', \tau) &= - \langle \Psi_0^N | \hat{\psi}^\dagger(\mathbf{r}') \hat{\psi}(\mathbf{r}) | \Psi_0^N \rangle W_p(\mathbf{r}, \mathbf{r}', \omega = 0) \\ &\quad + \frac{1}{2} \delta(\mathbf{r} - \mathbf{r}') W_p(\mathbf{r}, \mathbf{r}, \omega = 0), \end{aligned} \quad (5)$$

where we used the anti-commutator relation for the field operators, i.e., $\hat{\psi}(\mathbf{r}') \hat{\psi}^\dagger(\mathbf{r}) + \hat{\psi}^\dagger(\mathbf{r}') \hat{\psi}(\mathbf{r}) = \delta(\mathbf{r} - \mathbf{r}')$. The first term on the right-hand side of Eq. (5) when combined with the HF exchange

part of the self-energy, i.e.,

$$\Sigma_x^{\text{HF}}(\mathbf{r}, \mathbf{r}', \tau) = -\langle \Psi_0^N | \hat{\psi}^\dagger(\mathbf{r}') \hat{\psi}(\mathbf{r}) | \Psi_0^N \rangle v(\mathbf{r}, \mathbf{r}'), \quad (6)$$

yields the screened-exchange self-energy. The second term on the right-hand side of Eq. (5) is the (static) Coulomb-hole self-energy since $W_p(\mathbf{r}, \mathbf{r}, \omega = 0)$ is the Coulomb potential at \mathbf{r} due to the Coulomb hole created by an electron present at \mathbf{r} .

We can express W_p as

$$W_p(\mathbf{r}, \mathbf{r}', \omega) = \iint d\mathbf{r}_1 d\mathbf{r}_2 v(\mathbf{r}, \mathbf{r}_1) \chi(\mathbf{r}_1, \mathbf{r}_2, \omega) v(\mathbf{r}_2, \mathbf{r}'), \quad (7)$$

where the (reducible) polarizability χ can be written as

$$\chi(\mathbf{r}, \mathbf{r}', \omega) = \sum_m \left[\frac{\rho_m(\mathbf{r}) \rho_m(\mathbf{r}')}{\omega - \Omega_m + i\eta} - \frac{\rho_m(\mathbf{r}) \rho_m(\mathbf{r}')}{\omega + \Omega_m - i\eta} \right], \quad (8)$$

in which Ω_m is a neutral excitation energy and ρ_m the corresponding transition density. The latter is defined as

$$\rho_m(\mathbf{r}) = \sum_i^{\text{occ}} \sum_a^{\text{virt}} (\mathbf{X} + \mathbf{Y})_{ia}^m \phi_i(\mathbf{r}) \phi_a(\mathbf{r}) \quad (9)$$

where ϕ_p are either the (real-valued) HF spatial orbitals ϕ_p^{HF} (for a COHSEX@HF calculation) or the (real-valued) scCOHSEX spatial orbitals ϕ_p^{COHSEX} , i.e., the eigenfunctions of the COHSEX Hamiltonian $\hat{H}^{\text{COHSEX}} = \hat{H}^{\text{HF}} + \hat{\Sigma}_c^{\text{COHSEX}}$. In the following, the index m labels the single excitations; i and j are occupied orbitals; a and b are unoccupied orbitals, while $p, q, r,$ and s indicate arbitrary orbitals.

The neutral excitation energies Ω_m and the transition amplitudes $(\mathbf{X} + \mathbf{Y})_m^{ia}$ are obtained from a random-phase approximation (RPA) calculation:

$$\begin{pmatrix} \mathbf{A} & \mathbf{B} \\ -\mathbf{B} & -\mathbf{A} \end{pmatrix} \begin{pmatrix} \mathbf{X}_m \\ \mathbf{Y}_m \end{pmatrix} = \Omega_m \begin{pmatrix} \mathbf{X}_m \\ \mathbf{Y}_m \end{pmatrix}, \quad (10)$$

where $(\mathbf{X}_m, \mathbf{Y}_m)^T$ is the eigenvector that corresponds to Ω_m , and

$$A_{ia,jb} = \delta_{ij}\delta_{ab}(\epsilon_a - \epsilon_i) + 2(ia|jb), \quad (11a)$$

$$B_{ia,jb} = 2(ia|bj), \quad (11b)$$

where ϵ_p are either the HF orbital energies ϵ_p^{HF} (for a COHSEX@HF calculation) or the scCOHSEX orbital energies $\epsilon_p^{\text{COHSEX}}$ (i.e., the eigenvalues of \hat{H}^{COHSEX}), and $(pq|rs)$ are the bare two-electron integrals defined as

$$(pq|rs) = \iint d\mathbf{r}d\mathbf{r}' \phi_p(\mathbf{r})\phi_q(\mathbf{r})v(\mathbf{r}, \mathbf{r}')\phi_r(\mathbf{r}')\phi_s(\mathbf{r}'). \quad (12)$$

While the GW self-energy is non-Hermitian and frequency dependent, the COHSEX self-energy is both static and Hermitian as can be verified from the expression one obtains by inserting Eq. (8) into Eq. (4b) (with W_p given by (7)):

$$\begin{aligned} \Sigma_c^{\text{COHSEX}}(\mathbf{r}, \mathbf{r}') = & \left[\langle \Psi_0^N | \hat{\psi}^\dagger(\mathbf{r}')\hat{\psi}(\mathbf{r}) | \Psi_0^N \rangle - \langle \Psi_0^N | \hat{\psi}(\mathbf{r})\hat{\psi}^\dagger(\mathbf{r}') | \Psi_0^N \rangle \right] \\ & \times \iint d\mathbf{r}_1 d\mathbf{r}_2 v(\mathbf{r}, \mathbf{r}_1) \sum_m \frac{\rho_m(\mathbf{r}_1)\rho_m(\mathbf{r}_2)}{\Omega_m} v(\mathbf{r}_2, \mathbf{r}'). \quad (13) \end{aligned}$$

Moreover, it is important to note that the COHSEX self-energy has no poles. More precisely, its denominator never vanishes since the Ω_m are real and positive for finite systems. Owing to the Hermiticity of the COHSEX self-energy, Ψ_0^N can be represented by a single Slater determinant. Following the Slater-Condon rules the matrix elements in the above equation can then be rewritten as sums of products of orbitals. We obtain

$$\begin{aligned} \Sigma_c^{\text{COHSEX}}(\mathbf{r}, \mathbf{r}') = & 2 \left[\sum_i^{\text{occ}} \phi_i(\mathbf{r})\phi_i(\mathbf{r}') - \sum_a^{\text{virt}} \phi_a(\mathbf{r})\phi_a(\mathbf{r}') \right] \\ & \times \iint d\mathbf{r}_1 d\mathbf{r}_2 v(\mathbf{r}, \mathbf{r}_1) \sum_m \frac{\rho_m(\mathbf{r}_1)\rho_m(\mathbf{r}_2)}{\Omega_m} v(\mathbf{r}_2, \mathbf{r}'). \quad (14) \end{aligned}$$

The matrix element $\Sigma_{c,pq}^{\text{COHSEX}} = \langle \phi_p | \Sigma_c^{\text{COHSEX}} | \phi_q \rangle$ can now be written as

$$\Sigma_{c,pq}^{\text{COHSEX}} = 2 \sum_m \left[\sum_i^{\text{occ}} \frac{[pi|m][qi|m]}{\Omega_m} - \sum_a^{\text{virt}} \frac{[pa|m][qa|m]}{\Omega_m} \right], \quad (15)$$

where the screened two-electron integrals are defined as

$$[pq|m] = \sum_{ia} (pq|ia)(\mathbf{X} + \mathbf{Y})_m^{ia}. \quad (16)$$

When COHSEX is performed using first-order perturbation with respect to HF, the perturbation is given by $\hat{H}^{\text{COHSEX}} - \hat{H}^{\text{HF}} = \hat{\Sigma}_c^{\text{COHSEX}}$. The perturbative COHSEX orbital energies can thus be obtained from

$$\epsilon_p^{\text{COHSEX}} = \epsilon_p^{\text{HF}} + \Sigma_{c,pp}^{\text{COHSEX}}(\epsilon_p^{\text{HF}}). \quad (17)$$

Instead, within scCOHSEX both the eigenvalues and eigenfunctions of the COHSEX Hamiltonian have to be calculated repeatedly until a self-consistent result is obtained.

2.2 G_0W_0

Given the difficulty of evaluating the GW self-energy mentioned before one often uses a perturbative approach called G_0W_0 in which the self-energy is calculated perturbatively with respect to a simpler zeroth-order Hamiltonian, such as a self-energy for which a self-consistent solution is more easily obtained. In this work we will use the HF Green's function as our zeroth-order Green's function. Its spectral representation is given by

$$G_{\text{HF}}(\mathbf{r}, \mathbf{r}', \omega) = \sum_p \frac{\phi_p^{\text{HF}}(\mathbf{r})\phi_p^{\text{HF}}(\mathbf{r}')}{\omega - \epsilon_p^{\text{HF}} - i\eta \text{sign}(\mu - \epsilon_p^{\text{HF}})}, \quad (18)$$

with μ the chemical potential. Within the G_0W_0 approximation, the frequency integral in Eq. (4a) can be performed analytically and one obtains the following matrix elements of the G_0W_0 self-

energy,

$$\Sigma_{c,pq}^{G_0W_0}(\omega) = 2 \sum_m \left[\sum_i^{\text{occ}} \frac{[pi|m]^{\text{HF}}[qi|m]^{\text{HF}}}{\omega - \epsilon_i^{\text{HF}} + \Omega_m^{\text{HF}} - i\eta} + \sum_a^{\text{virt}} \frac{[pa|m]^{\text{HF}}[qa|m]^{\text{HF}}}{\omega - \epsilon_a^{\text{HF}} - \Omega_m^{\text{HF}} + i\eta} \right], \quad (19)$$

where the superscript in Ω_m^{HF} and $[pq|m]^{\text{HF}}$ indicates that these quantities are obtained from HF eigenvalues and orbitals. Contrary to the COHSEX self-energy, the above self-energy is dynamical and has poles. The QP energies can then be obtained from the poles of G obtained by solving the Dyson equation (2) (in frequency space) with the above self-energy. This yields the so-called QP equation,

$$\omega = \epsilon_p^{\text{HF}} + \text{Re}[\Sigma_{c,pp}^{G_0W_0}(\omega)]. \quad (20)$$

Due to the frequency dependence of the self-energy, the G_0W_0 QP equation has, in general, multiple solutions $\epsilon_{p,s}^{G_0W_0}$. The solution $\epsilon_p^{G_0W_0} \equiv \epsilon_{p,s=0}^{G_0W_0}$ with the largest spectral weight $Z_p(\epsilon_{p,s=0}^{G_0W_0})$ with

$$Z_p(\omega) = \left[1 - \frac{\text{Re}[\Sigma_{c,pp}^{G_0W_0}(\omega)]}{\partial\omega} \right]^{-1}, \quad (21)$$

is called the QP solution (or simply quasi-particle), while the other solutions ($s > 0$) are called satellites and share the rest of the spectral weight. In practice the QP equation is often simplified by Taylor expanding the self-energy to first order around ϵ_p^{HF} . The result is the so-called linearized QP equation given by

$$\epsilon_p^{G_0W_0} = \epsilon_p^{\text{HF}} + Z_p(\epsilon_p^{\text{HF}}) \text{Re}[\Sigma_{c,pp}^{G_0W_0}(\epsilon_p^{\text{HF}})]. \quad (22)$$

When the self-energy has poles close to a solution of the QP equation the above linearization is not justified. Moreover, it leads to irregularities in physical observables such as PES. This can be understood as follows.

Although the self-energy in the linearized QP equation is independent of the frequency its denominator could still vanish. This happens when $\epsilon_p^{\text{HF}} = \epsilon_i^{\text{HF}} - \Omega_m^{\text{HF}}$ or when $\epsilon_p^{\text{HF}} = \epsilon_a^{\text{HF}} + \Omega_m^{\text{HF}}$. When calculating a single QP for a single configuration of an atom or a molecule it is not very probable that such an event occurs. However, when a large number of QPs and/or configurations

is considered, e.g., when calculating a PES, it becomes inevitable. As an example, let us consider the simplest PES, namely the variation of the total energy of a diatomic molecule as a function of the interatomic distance R . In such a case, ϵ_p^{HF} and Ω_m^{HF} could be considered functions of R and the conditions that the self-energy has a vanishing denominator can be written as

$$\epsilon_p^{\text{HF}}(R) = \epsilon_i^{\text{HF}}(R) - \Omega_m^{\text{HF}}(R), \quad (23a)$$

$$\epsilon_p^{\text{HF}}(R) = \epsilon_a^{\text{HF}}(R) + \Omega_m^{\text{HF}}(R). \quad (23b)$$

Therefore, $\Sigma_{c,pp}^{G_0W_0}[\epsilon_p^{\text{HF}}(R)]$ can be considered an implicit function of R that has poles. From the above conditions it is clear that in a region equal to $2\Omega_0^{\text{HF}}(R) + \epsilon_{\text{LUMO}}^{\text{HF}}(R) - \epsilon_{\text{HOMO}}^{\text{HF}}(R)$ around the Fermi level no poles can occur, where Ω_0^{HF} is the smallest neutral excitation energy and $\epsilon_{\text{LUMO}}^{\text{HF}}$ and $\epsilon_{\text{HOMO}}^{\text{HF}}$ are the HF energies of the lowest unoccupied molecular orbital (LUMO) and the highest occupied molecular orbital (HOMO), respectively. However, since, in general, the variation with respect to R of the left- and right-hand sides of Eqs. (23a) and (23b) is different, it is unavoidable that outside of this range one of the two above conditions is met for some values $R = R_p$. We note that they can never be met simultaneously. In the vicinity of these R_p values the self-energy [see Eq. (19)] and its corresponding renormalization factor Z_p [see Eq. (21)] vary rapidly leading to irregularities in the QP energies and, hence, in the PES.

2.3 Partially self-consistent GW

The main drawback of the G_0W_0 approach is its dependence on the starting point, i.e., the orbitals and energies of the zeroth-order Hamiltonian. Since, as mentioned before, from a numerical point of view, fully self-consistent GW is nontrivial, so-called partial self-consistent GW methods have been developed to reduce or eliminate the starting-point dependence. Within evGW one only updates the eigenvalues in the self-energy while in qsGW one symmetrizes the G_0W_0 self-energy according to

$$\Sigma_{c,pq}^{\text{qsGW}} = \frac{1}{2} \text{Re} \left[\Sigma_{c,pq}^{G_0W_0}(\epsilon_p^{\text{qsGW}}) + \Sigma_{c,pq}^{G_0W_0}(\epsilon_q^{\text{qsGW}}) \right]. \quad (24)$$

The above self-energy is frequency-independent and Hermitian and is, hence, suitable for a standard self-consistent procedure. Therefore, in this partially self-consistent scheme both the eigenvalues and orbitals are updated.

However, the *evGW* and *qsGW* approaches suffer from the same problem as G_0W_0 since the self-energies have poles when considered as (implicit) functions of the geometry. In fact the problem is even more severe since, due to the self-consistent procedure, an irregularity in one QP energy is transferred to all the other QP energies. As a consequence, in some regions of the geometry space, there is more than one branch of solutions and discontinuities appear when a solution switches from one branch to another.^{40,41}

2.4 Correlation energy

We calculate the correlation energies at the BSE level using an approach based on the ACFDT.⁴³⁻⁴⁵ We note that the ACFDT formalism is formally derived for a local potential, while here the potential, i.e., the self-energy, is non-local. We strictly follow the ACFDT procedure described in Ref. 42 and the details can be found there. For the sake of completeness we briefly discuss some details of the calculation of the BSE total energy. The main difference with Ref. 42 is that the QP energies and orbitals appearing in the equations below are those pertaining to the COHSEX self-energy instead of the G_0W_0 self-energy.

Within the ACFDT formalism, the BSE correlation energy can be written as an integral over the coupling constant λ which adiabatically connects the noninteracting system ($\lambda = 0$) with the fully interacting system ($\lambda = 1$) according to^{42,49-53}

$$E_c^{\text{BSE}} = \frac{1}{2} \int_0^1 \text{Tr} \left(\mathbf{K} \mathbf{P}^\lambda \right) d\lambda \quad (25)$$

where the polarizability matrix \mathbf{P}^λ is given by

$$\mathbf{P}^\lambda = \begin{pmatrix} \mathbf{Y}^\lambda (\mathbf{Y}^\lambda)^T & \mathbf{Y}^\lambda (\mathbf{X}^\lambda)^T \\ \mathbf{X}^\lambda (\mathbf{Y}^\lambda)^T & \mathbf{X}^\lambda (\mathbf{X}^\lambda)^T \end{pmatrix} - \begin{pmatrix} \mathbf{0} & \mathbf{0} \\ \mathbf{0} & \mathbf{1} \end{pmatrix} \quad (26)$$

with \mathbf{X}^λ and \mathbf{Y}^λ solutions of

$$\begin{pmatrix} \mathbf{A}^{\lambda,\text{BSE}} & \mathbf{B}^{\lambda,\text{BSE}} \\ -\mathbf{B}^{\lambda,\text{BSE}} & -\mathbf{A}^{\lambda,\text{BSE}} \end{pmatrix} \begin{pmatrix} \mathbf{X}_m^\lambda \\ \mathbf{Y}_m^\lambda \end{pmatrix} = \Omega_m^\lambda \begin{pmatrix} \mathbf{X}_m^\lambda \\ \mathbf{Y}_m^\lambda \end{pmatrix}, \quad (27)$$

where

$$A_{ia,jb}^{\lambda,\text{BSE}} = \delta_{ij}\delta_{ab}(\epsilon_a - \epsilon_i) + \lambda \left[2(ia|jb) - W_{ij,ab}^\lambda \right], \quad (28)$$

$$B_{ia,jb}^{\lambda,\text{BSE}} = \lambda \left[2(ia|bj) - W_{ib,aj}^\lambda \right], \quad (29)$$

with

$$W_{pq,rs}^\lambda = \iint d\mathbf{r}d\mathbf{r}' \phi_p(\mathbf{r})\phi_q(\mathbf{r})W^\lambda(\mathbf{r},\mathbf{r}',\omega=0)\phi_r(\mathbf{r}')\phi_s(\mathbf{r}'), \quad (30)$$

Finally, the interaction kernel \mathbf{K} is given by

$$\mathbf{K} = \begin{pmatrix} \tilde{\mathbf{A}}^{\text{BSE}} & \mathbf{B}^{\lambda=1,\text{BSE}} \\ \mathbf{B}^{\lambda=1,\text{BSE}} & \tilde{\mathbf{A}}^{\text{BSE}} \end{pmatrix} \quad (31)$$

with $\tilde{A}_{ia,jb}^{\text{BSE}} = 2(ia|bj)$. We note that Eq. (25) is referred to as “extended Bethe-Salpeter (XBS)” in Ref. 51. An important point to make here is that, in contrast to Kohn-Sham density-functional theory where the electron density is fixed along the adiabatic path,^{43,44} the density is not maintained in the present BSE formalism as the coupling constant varies. Therefore, an additional contribution to Eq. (25) originating from the variation of the Green’s function along the adiabatic connection path should be, in principle, added.⁶⁹ However, as it is commonly done,^{46,47,51,70} we shall neglect it in the present study.

The BSE total energy E^{BSE} of the system can then be written as

$$E^{\text{BSE}} = E^{\text{nuc}} + E^{\text{HF}} + E_c^{\text{BSE}} \quad (32)$$

where E^{nuc} and E^{HF} are the nuclear energy and the HF energy, respectively. We note that for a BSE@scCOHSEX calculation E^{HF} is calculated with the scCOHSEX orbitals.

3 Results

All systems under investigation have a closed-shell singlet ground state. Hence, the restricted HF formalism has been systematically employed in the present study. Finally, the infinitesimal η is set to zero for all calculations. The numerical integration required to compute the correlation energy along the adiabatic path [see Eq. (25)] is performed with a 21-point Gauss-Legendre quadrature. All the calculations have been performed with the software QUACK,⁷¹ freely available on `github`. As one-electron basis sets, we employ the Dunning family (cc-pVXZ) defined with cartesian Gaussian functions.

3.1 Irregularities and discontinuities in G_0W_0 , evGW, and qsGW

We have previously described in detail the problem of irregularities and discontinuities in physical observables obtained from G_0W_0 and partially self-consistent GW approaches.^{40,41} Here we want to remind the reader that these problems are also present in total energy calculations and we want to show that, instead, there are no such problems in the COHSEX method. In Fig. 1 we report the BSE total energy of the LiF molecule as a function of the interatomic distance in the vicinity of its equilibrium distance. The BSE correlation energy is calculated on top of G_0W_0 @HF, COHSEX@HF, evGW@HF, qsGW, and scCOHSEX. We used a relatively small basis set, namely Dunning’s cc-pVDZ basis, since for larger basis sets the qsGW approach does not yield converged results for many values of R . This, however, does not change the conclusions of this section. We note that within qsGW the entire set of energies and orbitals is updated at each iteration. We

see that all four results are within a range of about 10 mHartree. However, the PES obtained from BSE@ G_0W_0 @HF shows irregularities while the PES obtained from BSE@evGW@HF and BSE@qsGW show discontinuities. In fact, the different branches of solutions can clearly be seen, especially around 3.4 bohr. Instead, the BSE total energies obtained on top of a COHSEX calculation, i.e., BSE@COHSEX@HF and BSE@scCOHSEX, yield a PES that is a smooth function of the interatomic distance.

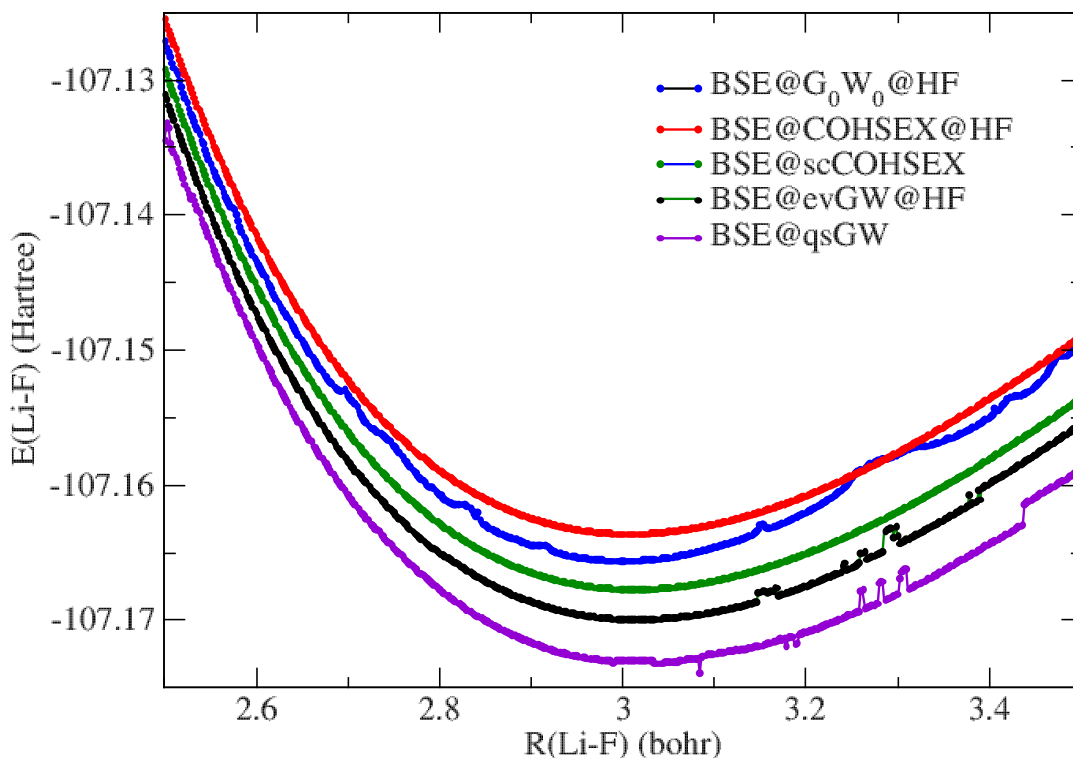


Figure 1: The BSE total energy of the LiF molecule in the cc-pVDZ basis as a function of the internuclear distance. The calculations were done at intervals of 0.002 bohr.

Finally, we note that including self-consistency in COHSEX and GW tends to lower the total energies and that including self-consistency for both QP energies and orbitals lowers the total energy more than just including self-consistency for the QP energies. Moreover, the effect of self-consistency on the total energies in COHSEX, going from COHSEX@HF to scCOHSEX, is

roughly identical to the effect on GW , going from $G_0W_0@HF$ to $evGW@HF$.

3.2 Ground-state PES

In Figs. 2-9 we report the BSE total energies as a function of the interatomic distance around the equilibrium distance for the following diatomic molecules: H_2 , LiH , LiF , HCl , N_2 , CO , BF , and F_2 , respectively. They are the same molecules that were studied in Ref. 42. We also use the same basis set, namely Dunning’s cc-pVQZ. For comparison we also report the PES obtained with the coupled cluster (CC) methods of increasing accuracy: CC2,⁷² CCSD,⁷³ CC3.⁷⁴ At the equilibrium distance the CC3 approach has been shown to yield total energies that are very close to those obtained with higher-order CC approaches, such as CCSDT and CCSDT(Q).⁴² Therefore, we can consider it to be the reference method.

In the only case for which we have an exact result (for the given basis set), namely the H_2 PES obtained from full configuration interaction (FCI), all BSE total energies are roughly the same. We also note that no irregularities are visible in the $BSE@G_0W_0@HF$ curve. In the case of LiH , the second smallest molecule in the set, an irregularity appears in the $BSE@G_0W_0@HF$ curve around 3.08 bohr. We also observe that the smooth $BSE@COHSEX@HF$ total-energy curves are closest to the reference CC3 values, while $BSE@scCOHSEX$ and $BSE@G_0W_0@HF$ yield almost identical energies. For the LiF molecule there are large irregularities in the PES obtained within $BSE@G_0W_0@HF$ around 2.9 bohr which impedes a straightforward determination of the equilibrium distance (see below). Another large irregularity appears around 3.4 bohr. Again the smooth $BSE@COHSEX@HF$ curve is closest to that obtained within CC3, although the differences with the $BSE@G_0W_0@HF$ results are small. Finally, similar to the LiF results obtained above for the small cc-pVDZ basis, we observe again that including self-consistency in the COHSEX calculation lowers the total energy, thereby worsening the agreement with the coupled-cluster reference data.

The PES of all diatomic molecules, except the smallest two (H_2 and LiH), show a similar trend, i.e., small differences between the $BSE@COHSEX@HF$ and $BSE@G_0W_0@HF$ total energies and

Table 1: Equilibrium distances (in bohr) obtained in the cc-pVQZ basis set. The experimental values are extracted from Ref. 75. The results in brackets for LiF and F₂ were obtained by fitting the total energies to a Morse potential since the irregularities in the PES precluded a direct evaluation.

	H ₂	LiH	LiF	HCl	N ₂	CO	BF	F ₂
CC3	1.402	3.019	2.963	2.403	2.075	2.136	2.390	2.663
BSE@G ₀ W ₀ @HF	1.399	3.017	(2.973)	2.400	2.065	2.134	2.385	(2.638)
BSE@COHSEX@HF	1.399	3.014	2.961	2.400	2.066	2.125	2.379	2.635
BSE@scCOHSEX	1.401	3.016	2.963	2.404	2.070	2.130	2.387	2.650
Experiment	1.401	3.015	2.948	2.409	2.074	2.132	2.386	2.668

a relatively large difference with respect to the BSE@scCOHSEX total energies. Therefore, we conclude that the self-consistency has a much larger influence on the PES than the difference in the COHSEX and GW self-energies.

The PES of the HCl, N₂, CO and BF molecules obtained within BSE@G₀W₀@HF all exhibit small irregularities, while those in F₂ are very large, preventing a simple determination of the F₂ equilibrium distance (see below). Again, BSE@COHSEX@HF is in excellent agreement with the CC3 results and even slightly better than those obtained within BSE@G₀W₀@HF, and, most importantly, the PES obtained within BSE@COHSEX@HF (and BSE@scCOHSEX) are devoid of irregularities and discontinuities.

In Table 1 we report the equilibrium distances obtained within the various BSE approaches and we compare them to the CC3 reference values and to experiment. As mentioned before, the irregularities in the PES can prevent a straightforward determination of the equilibrium distance. Therefore, following Ref. 42, for LiF and F₂ a Morse potential was used to fit the total energies in order to estimate the equilibrium distance. Although the total energies obtained within BSE@scCOHSEX were not as accurate as those obtained using perturbative QP energies, adding self-consistency to the COHSEX approach improves the equilibrium distances. In summary, while BSE@COHSEX@HF yields the smallest errors for the total energies, BSE@scCOHSEX yields the smallest errors for the equilibrium distances.

Finally, in order to estimate the influence of the QP energies on the BSE total energies, we report

the ionization potentials (IP) and the HOMO-LUMO gaps at the equilibrium distance corresponding to each level of theory for the various BSE approaches in Tables 2 and 3, respectively, and we compare to experimental data (when available). For the IP we also report the CCSD(T)/def2TZVPP data of Ref. 76 which are in good agreement with the experimental values with the exception of H₂. Comparing the differences in the IP with the differences in the PES, there does not emerge a clear link between the two. Although the IP obtained within COHSEX@HF and G₀W₀@HF show the largest differences (except for N₂), the differences between the corresponding BSE total energies are the smallest. Instead, the differences in the IP between scCOHSEX and COHSEX@HF are the smallest (except for N₂) but the differences in the corresponding total energies are the largest. A similar analysis holds for the HOMO-LUMO gaps. Moreover, despite the fact that COHSEX@HF yields IP and HOMO-LUMO gaps significantly worse than those obtained within G₀W₀@HF when compared to the experimental values, the corresponding BSE total energies are very similar (except for the irregularities in G₀W₀@HF@BSE). Therefore, at least for the small molecules discussed here, the BSE total energies obtained within ACFDT seem to be robust with respect to the underlying QP energies. Instead, the total energies are sensitive to the screening that enters the BSE. Within BSE@COHSEX@HF and BSE@G₀W₀@HF this quantity is identical since in both cases it is calculated from the HF orbitals and energies. However, when one includes self-consistency, the screening changes and it has a significant influence on the total energy. We can therefore conclude that the screened Coulomb potential is the key quantity in the calculation of correlation energies within the ACFDT@BSE formalism, and ultimately dictates the accuracy of the total energy.

4 Conclusions

We have demonstrated that COHSEX is a promising approach to obtain quasi-particle energies for the calculation of potential energy surfaces. Contrary to G₀W₀ and partially self-consistent GW approaches, COHSEX yields results without irregularities and discontinuities. We have

Table 2: Ionization potentials (in eV) at the equilibrium distance obtained in the cc-pVQZ basis set except for the CCSD(T) values from Ref. 76 which have been obtained in the def2-TZVPP basis. The experimental values are extracted from Ref. 18

	H ₂	LiH	LiF	HCl	N ₂	CO	BF	F ₂
G ₀ W ₀ @HF	16.57	8.26	11.59	12.98	17.33	14.91	11.41	16.50
COHSEX@HF	18.05	9.52	13.82	14.49	19.48	16.69	12.86	18.88
scCOHSEX	17.83	9.21	13.12	14.02	17.52	15.79	12.45	18.00
CCSD(T)	16.40	7.96	11.32	12.59	15.57	14.21	11.09	15.71
Experiment	15.43	7.90	11.30	12.79	15.58	14.01	11.00	15.70

Table 3: HOMO-LUMO gaps (in eV) at the equilibrium distance obtained in the cc-pVQZ basis set. The experimental values are extracted from Ref. 50

	H ₂	LiH	LiF	HCl	N ₂	CO	BF	F ₂
G ₀ W ₀ @HF	20.24	8.04	11.31	15.20	20.24	17.33	12.90	17.32
COHSEX@HF	21.59	9.27	13.54	16.45	21.38	18.44	13.97	18.14
scCOHSEX	21.57	8.99	12.84	16.07	20.09	17.93	13.73	17.81
Experiment		8.24						16.94

illustrated this feature by calculating the ground-state potential energy surfaces of diatomic molecules. Moreover, we have shown that BSE total energies of diatomic molecules using COHSEX quasi-particle energies obtained perturbatively on top of a Hartree-Fock calculation are in good agreement with accurate coupled-cluster results. Finally, we showed that including self-consistency in the COHSEX approach for both quasi-particle energies and orbitals, in order to make the results independent of the starting point, worsens the total energies but improves the equilibrium distances. This is mainly due to variations in the screening W that enters the BSE.

Acknowledgement

JAB and PR thank the French Agence Nationale de la Recherche (ANR) for financial support (Grant agreements ANR-18-CE30-0025 and ANR-19-CE30-0011). PFL thanks the European Research

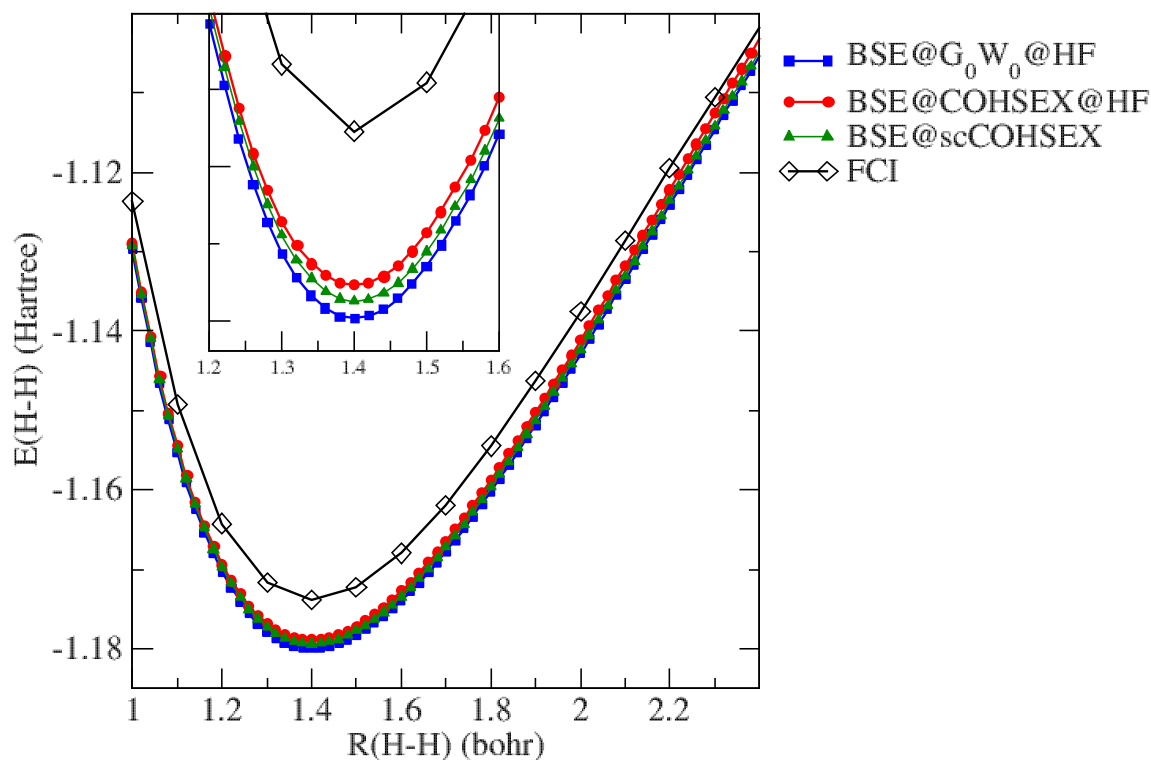


Figure 2: The total energy of the H₂ molecule in the cc-pVQZ basis as a function of the internuclear distance.

Council (ERC) under the European Union’s Horizon 2020 research and innovation programme (Grant agreement No. 863481) for financial support. This study has also been partially supported through the EUR grant NanoX n^o ANR-17-EURE-0009 in the framework of the “Programme des Investissements d’Avenir”.

References

- (1) Hedin, L. New Method for Calculating the One-Particle Green’s Function with Application to the Electron-Gas Problem. *Phys. Rev.* **1965**, *139*, A796.

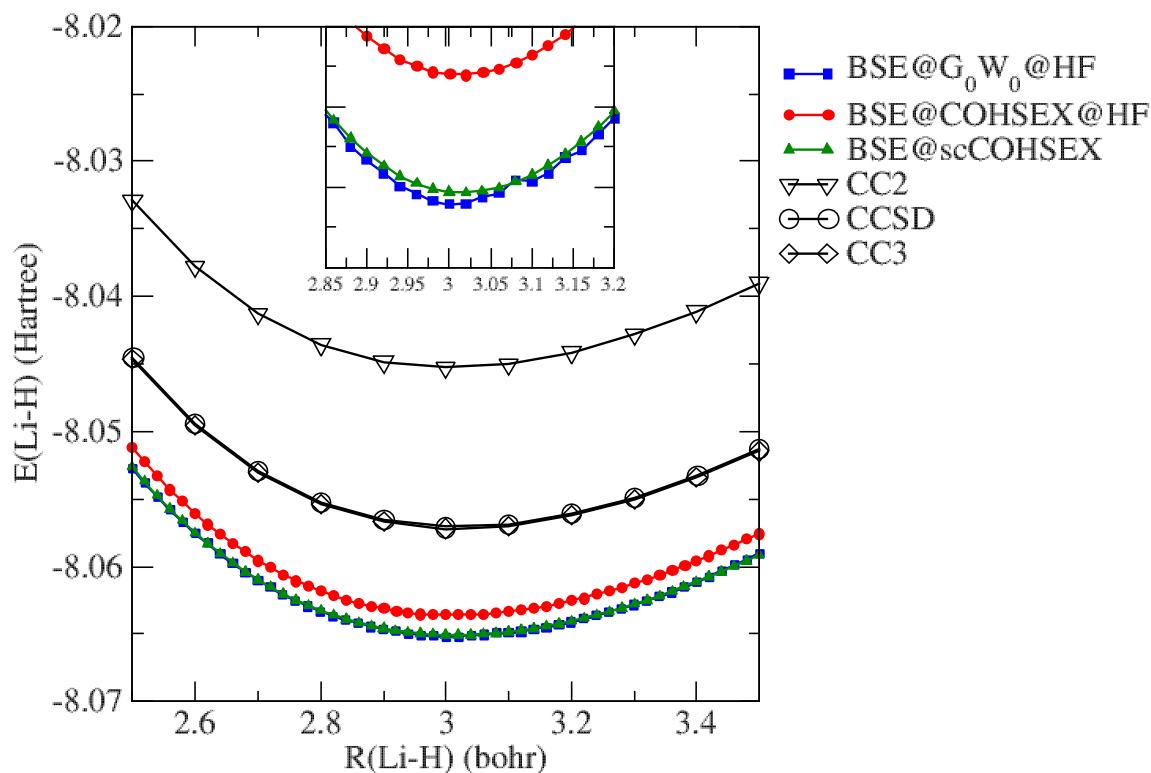


Figure 3: The total energy of the LiH molecule in the cc-pVQZ basis as a function of the internuclear distance.

- (2) Aryasetiawan, F.; Gunnarsson, O. The GW method. *Rep. Prog. Phys.* **1998**, *61*, 237–312.
- (3) Reining, L. The GW Approximation: Content, Successes and Limitations: The GW Approximation. *Wiley Interdiscip. Rev. Comput. Mol. Sci.* **2017**, e1344.
- (4) Golze, D.; Dvorak, M.; Rinke, P. The GW Compendium: A Practical Guide to Theoretical Photoemission Spectroscopy. *Frontiers in Chemistry* **2019**, *7*, 377.
- (5) Stan, A.; Dahlen, N. E.; van Leeuwen, R. Fully Self-Consistent GW Calculations for Atoms and Molecules. *Europhys. Lett. EPL* **2006**, *76*, 298–304.

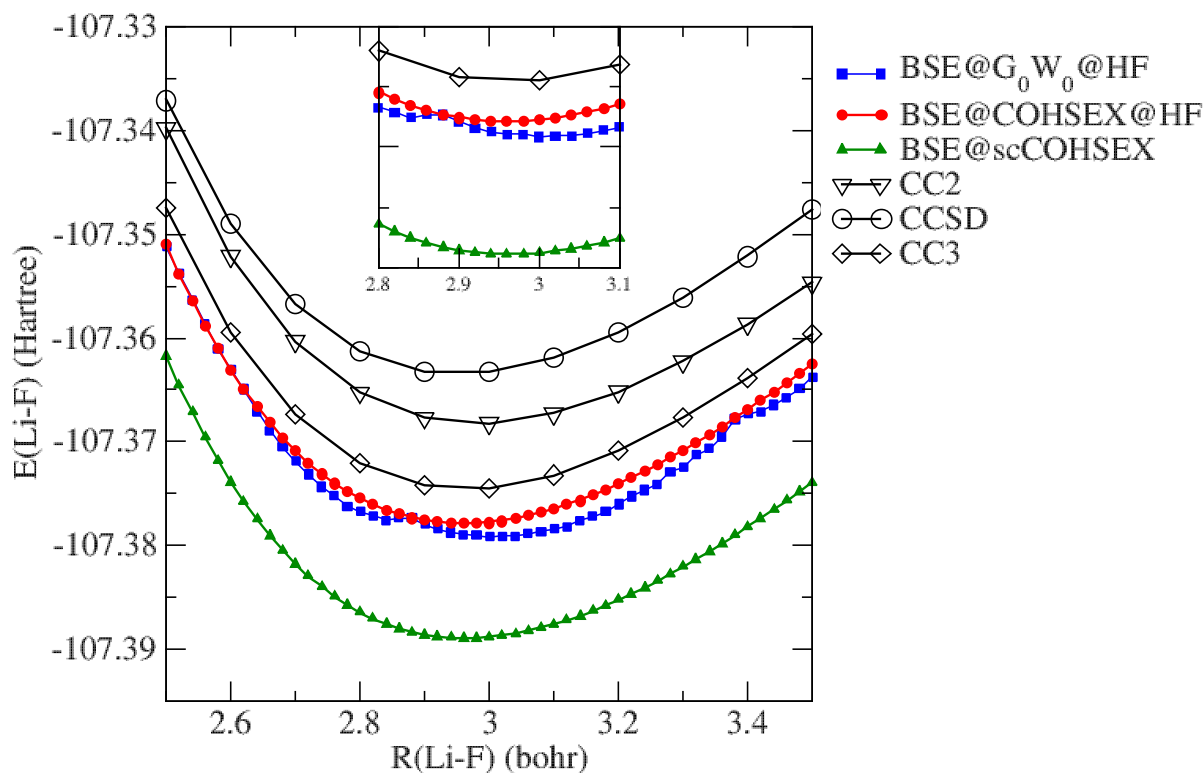


Figure 4: The total energy of the LiF molecule in the cc-pVQZ basis as a function of the internuclear distance.

- (6) Stan, A.; Dahlen, N. E.; van Leeuwen, R. Levels of Self-Consistency in the GW Approximation. *J. Chem. Phys.* **2009**, *130*, 114105.
- (7) Rostgaard, C.; Jacobsen, K. W.; Thygesen, K. S. Fully Self-Consistent GW Calculations for Molecules. *Phys. Rev. B* **2010**, *81*, 085103.
- (8) Caruso, F.; Rinke, P.; Ren, X.; Scheffler, M.; Rubio, A. Unified Description of Ground and Excited States of Finite Systems: The Self-Consistent G W Approach. *Phys. Rev. B* **2012**, *86*, 081102(R).
- (9) Caruso, F.; Rohr, D. R.; Hellgren, M.; Ren, X.; Rinke, P.; Rubio, A.; Scheffler, M. Bond Breaking

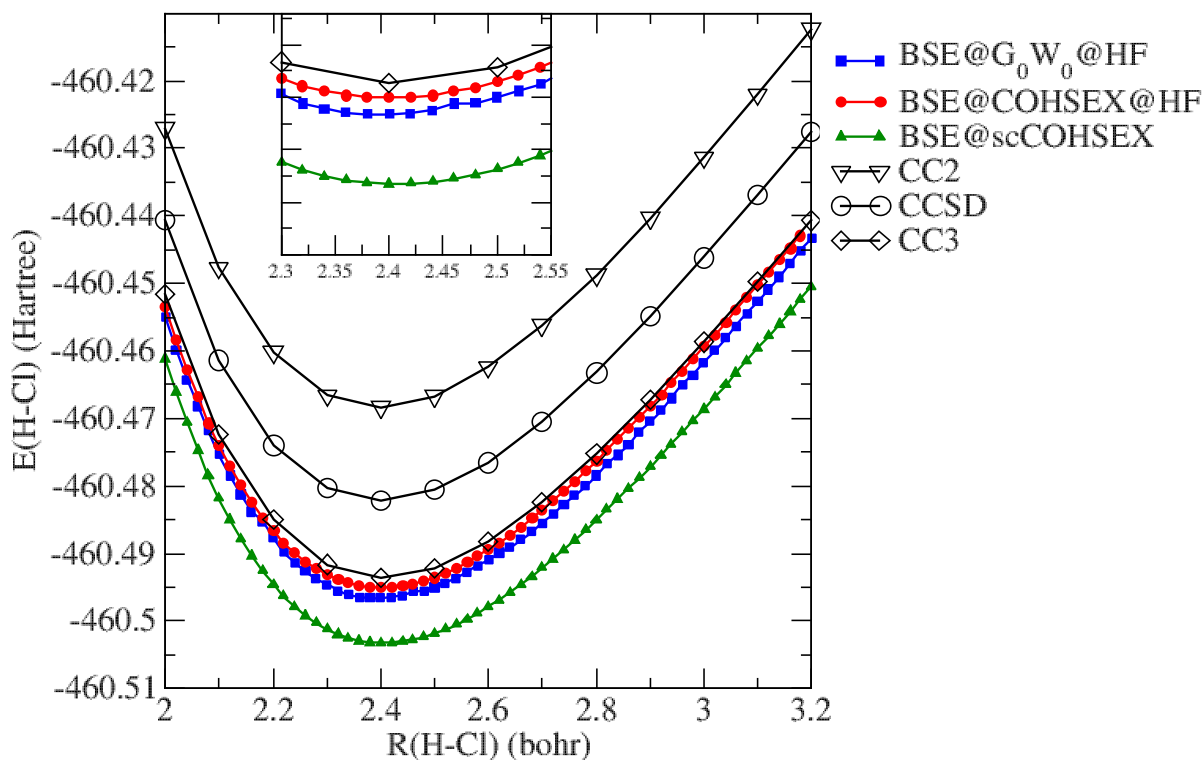


Figure 5: The total energy of the HCl molecule in the cc-pVQZ basis as a function of the internuclear distance.

and Bond Formation: How Electron Correlation Is Captured in Many-Body Perturbation Theory and Density-Functional Theory. *Phys. Rev. Lett.* **2013**, *110*, 146403.

(10) Caruso, F.; Rinke, P.; Ren, X.; Rubio, A.; Scheffler, M. Self-Consistent G W : All-Electron Implementation with Localized Basis Functions. *Phys. Rev. B* **2013**, *88*, 075105.

(11) Caruso, F. Self-Consistent GW Approach for the Unified Description of Ground and Excited States of Finite Systems. PhD Thesis, Freie Universität Berlin, 2013.

(12) Koval, P.; Foerster, D.; Sánchez-Portal, D. Fully Self-Consistent G W and Quasiparticle Self-Consistent G W for Molecules. *Phys. Rev. B* **2014**, *89*, 155417.

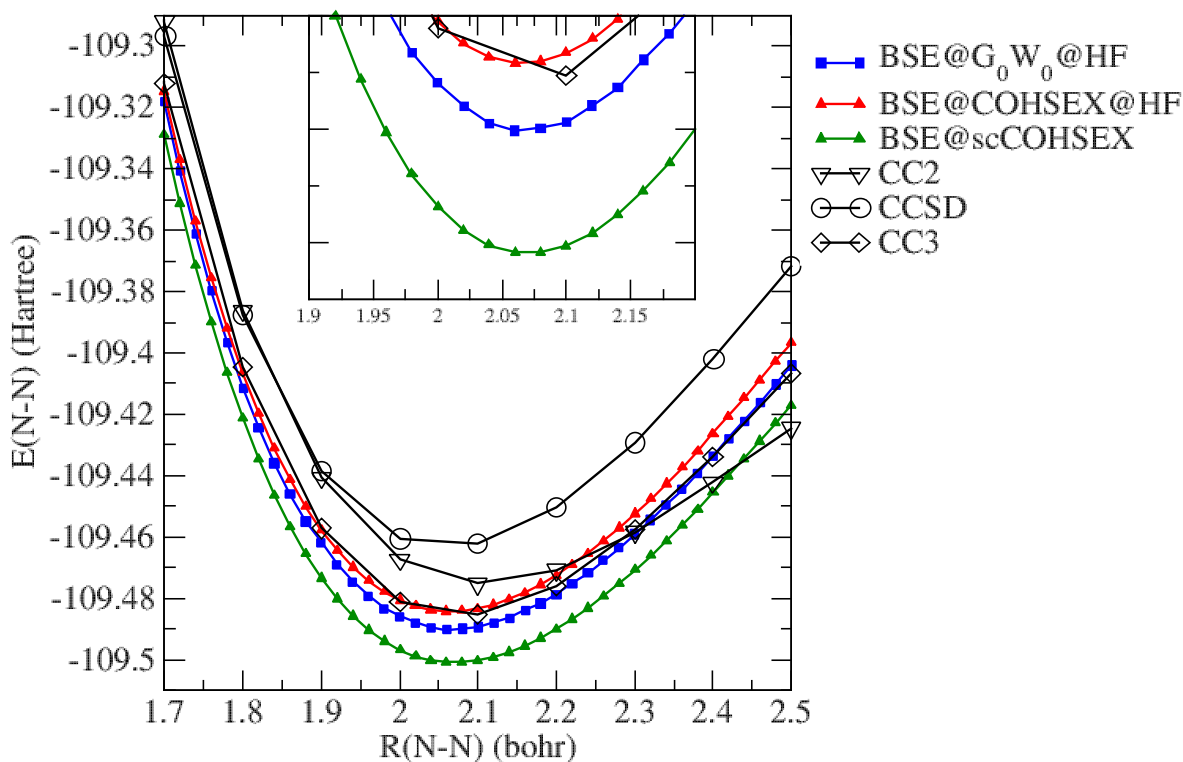


Figure 6: The total energy of the N_2 molecule in the cc-pVQZ basis as a function of the internuclear distance.

- (13) Wilhelm, J.; Golze, D.; Talirz, L.; Hutter, J.; Pignedoli, C. A. Toward *GW* Calculations on Thousands of Atoms. *J. Phys. Chem. Lett.* **2018**, *9*, 306–312.
- (14) Hybertsen, M. S.; Louie, S. G. First-Principles Theory of Quasiparticles: Calculation of Band Gaps in Semiconductors and Insulators. *Phys. Rev. Lett.* **1985**, *55*, 1418–1421.
- (15) van Setten, M. J.; Weigend, F.; Evers, F. The *GW* -Method for Quantum Chemistry Applications: Theory and Implementation. *J. Chem. Theory Comput.* **2013**, *9*, 232–246.
- (16) Bruneval, F. Ionization Energy of Atoms Obtained from *GW* Self-Energy or from Random Phase Approximation Total Energies. *J. Chem. Phys.* **2012**, *136*, 194107.

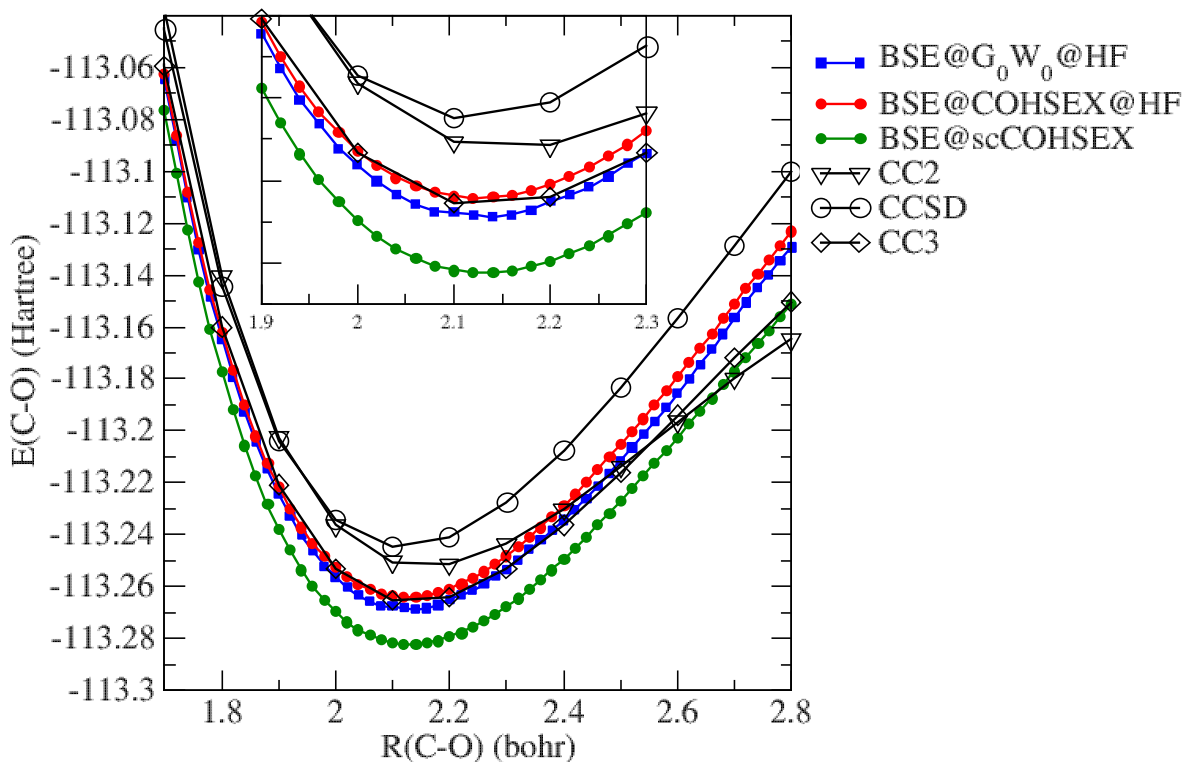


Figure 7: The total energy of the CO molecule in the cc-pVQZ basis as a function of the internuclear distance.

- (17) Bruneval, F.; Marques, M. A. L. Benchmarking the Starting Points of the GW Approximation for Molecules. *J. Chem. Theory Comput.* **2013**, *9*, 324–329.
- (18) van Setten, M. J.; Caruso, F.; Sharifzadeh, S.; Ren, X.; Scheffler, M.; Liu, F.; Lischner, J.; Lin, L.; Deslippe, J. R.; Louie, S. G.; Yang, C.; Weigend, F.; Neaton, J. B.; Evers, F.; Rinke, P. GW 100: Benchmarking $G_0 W_0$ for Molecular Systems. *J. Chem. Theory Comput.* **2015**, *11*, 5665–5687.
- (19) van Setten, M. J.; Costa, R.; Viñes, F.; Illas, F. Assessing GW Approaches for Predicting Core Level Binding Energies. *J. Chem. Theory Comput.* **2018**, *14*, 877–883.
- (20) Hybertsen, M. S.; Louie, S. G. Electron Correlation in Semiconductors and Insulators: Band Gaps and Quasiparticle Energies. *Phys. Rev. B* **1986**, *34*, 5390–5413.

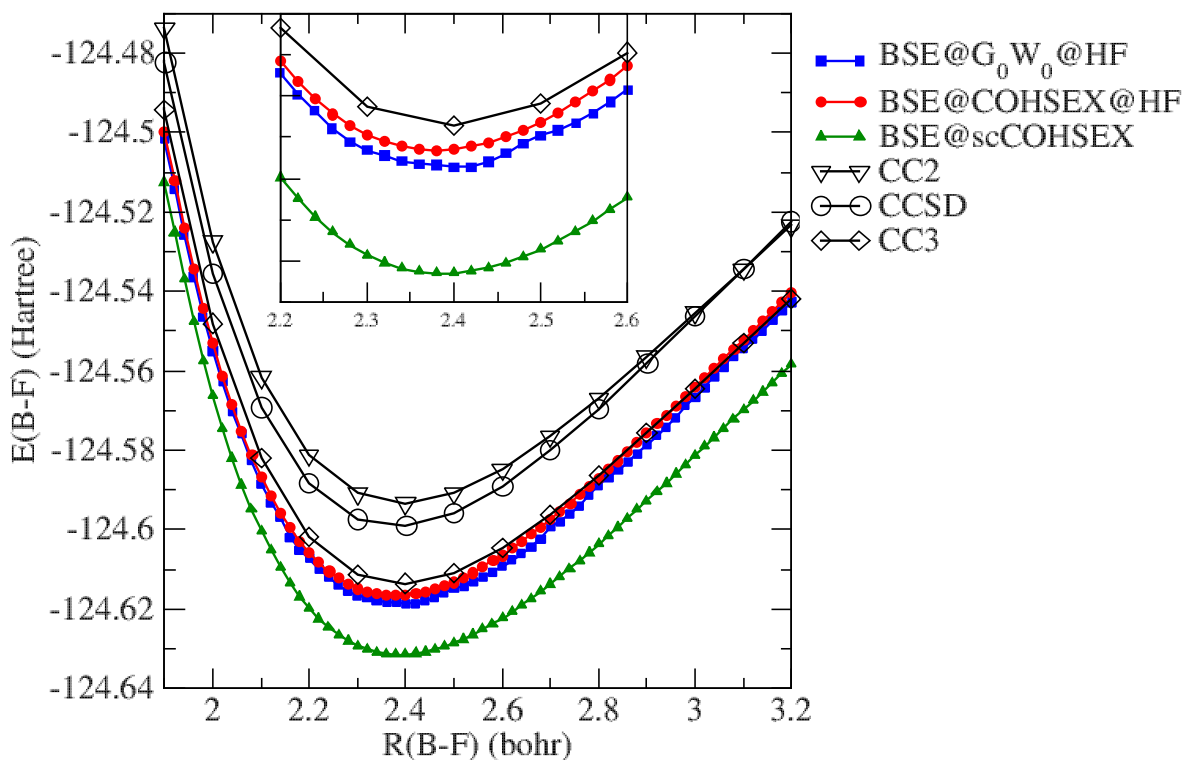


Figure 8: The total energy of the BF molecule in the cc-pVQZ basis as a function of the internuclear distance.

- (21) Shishkin, M.; Kresse, G. Self-Consistent G W Calculations for Semiconductors and Insulators. *Phys. Rev. B* **2007**, *75*, 235102.
- (22) Blase, X.; Attaccalite, C.; Olevano, V. First-Principles GW Calculations for Fullerenes, Porphyrins, Phtalocyanine, and Other Molecules of Interest for Organic Photovoltaic Applications. *Phys. Rev. B* **2011**, *83*, 115103.
- (23) Faber, C.; Attaccalite, C.; Olevano, V.; Runge, E.; Blase, X. First-Principles GW Calculations for DNA and RNA Nucleobases. *Phys. Rev. B* **2011**, *83*, 115123.
- (24) Faleev, S. V.; van Schilfgarde, M.; Kotani, T. All-Electron Self-Consistent G W Approximation: Application to Si, MnO, and NiO. *Phys. Rev. Lett.* **2004**, *93*, 126406.

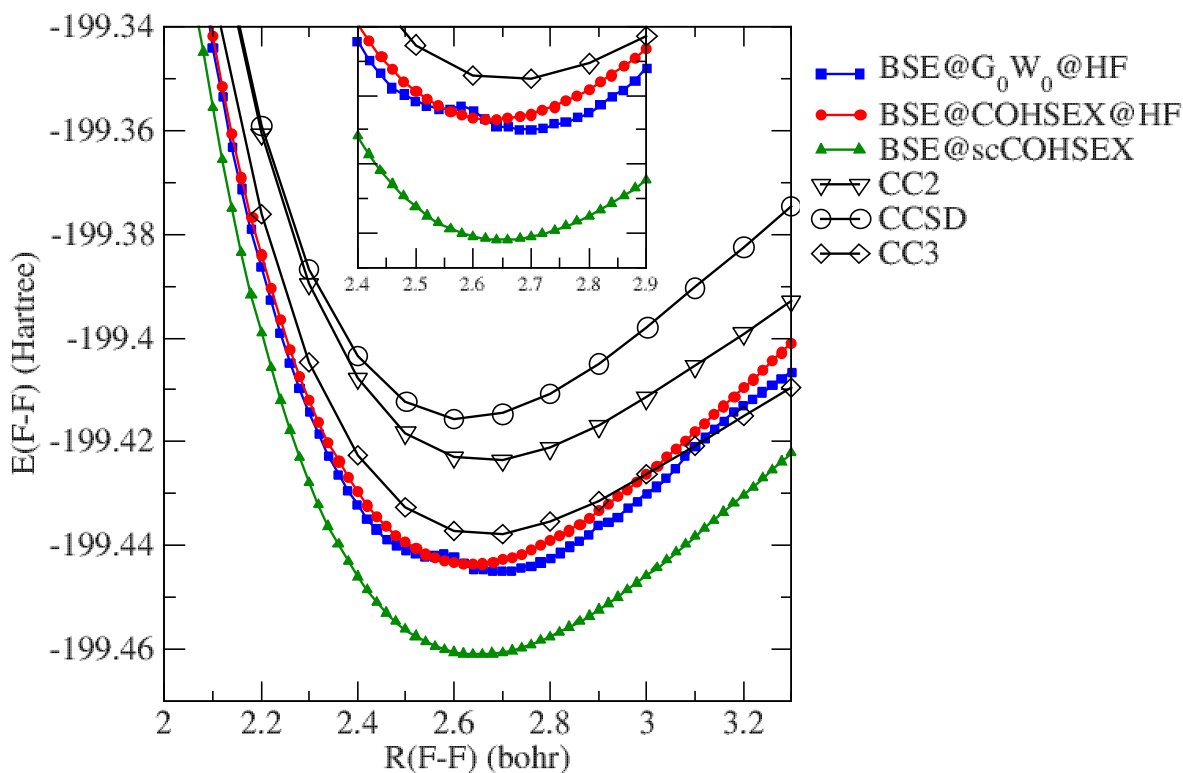


Figure 9: The total energy of the F_2 molecule in the cc-pVQZ basis as a function of the internuclear distance.

- (25) van Schilfgaarde, M.; Kotani, T.; Faleev, S. Quasiparticle Self-Consistent G W Theory. *Phys. Rev. Lett.* **2006**, *96*, 226402.
- (26) Kotani, T.; van Schilfgaarde, M.; Faleev, S. V. Quasiparticle Self-Consistent G W Method: A Basis for the Independent-Particle Approximation. *Phys. Rev. B* **2007**, *76*, 165106.
- (27) Ke, S.-H. All-Electron G W Methods Implemented in Molecular Orbital Space: Ionization Energy and Electron Affinity of Conjugated Molecules. *Phys. Rev. B* **2011**, *84*, 205415.
- (28) Kaplan, F.; Harding, M. E.; Seiler, C.; Weigend, F.; Evers, F.; van Setten, M. J. Quasi-Particle Self-Consistent GW for Molecules. *J. Chem. Theory Comput.* **2016**, *12*, 2528–2541.

- (29) Rangel, T.; Hamed, S. M.; Bruneval, F.; Neaton, J. B. Evaluating the GW Approximation with CCSD(T) for Charged Excitations Across the Oligoacenes. *J. Chem. Theory Comput.* **2016**, *12*, 2834–2842.
- (30) Caruso, F.; Dauth, M.; van Setten, M. J.; Rinke, P. Benchmark of GW Approaches for the GW100 Test Set. *J. Chem. Theory Comput.* **2016**, *12*, 5076.
- (31) Romaniello, P.; Guyot, S.; Reining, L. The Self-Energy beyond GW: Local and Nonlocal Vertex Corrections. *J. Chem. Phys.* **2009**, *131*, 154111.
- (32) Romaniello, P.; Bechstedt, F.; Reining, L. Beyond the G W Approximation: Combining Correlation Channels. *Phys. Rev. B* **2012**, *85*, 155131.
- (33) Berger, J. A.; Romaniello, P.; Tandetzky, F.; Mendoza, B. S.; Brouder, C.; Reining, L. Solution to the Many-Body Problem in One Point. *New J. Phys.* **2014**, *16*, 113025.
- (34) Stan, A.; Romaniello, P.; Rigamonti, S.; Reining, L.; Berger, J. A. Unphysical and physical solutions in many-body theories: from weak to strong correlation. *New J. Phys.* **2015**, *17*, 093045.
- (35) Di Sabatino, S.; Berger, J. A.; Reining, L.; Romaniello, P. Reduced density-matrix functional theory: Correlation and spectroscopy. *J. Chem. Phys.* **2015**, *143*, 024108.
- (36) Di Sabatino, S.; Berger, J. A.; Reining, L.; Romaniello, P. Photoemission Spectra from Reduced Density Matrices: The Band Gap in Strongly Correlated Systems. *Physical Review B* **2016**, *94*, 155141.
- (37) Tarantino, W.; Romaniello, P.; Berger, J. A.; Reining, L. Self-Consistent Dyson Equation and Self-Energy Functionals: An Analysis and Illustration on the Example of the Hubbard Atom. *Phys. Rev. B* **2017**, *96*, 045124.

- (38) Tarantino, W.; Mendoza, B. S.; Romaniello, P.; Berger, J. A.; Reining, L. Many-body perturbation theory and non-perturbative approaches: screened interaction as the key ingredient. *J. Phys.: Condensed Matter* **2018**, *30*, 135602.
- (39) Di Sabatino, S.; Koskelo, J.; Berger, J. A.; Romaniello, P. *arXiv:2002.11198*
- (40) Loos, P. F.; Romaniello, P.; Berger, J. A. Green functions and self-consistency: insights from the spherium model. *J. Chem. Theory Comput.* **2018**, *14*, 3071–3082.
- (41) V eril, M.; Romaniello, P.; Berger, J. A.; Loos, P.-F. Unphysical Discontinuities in GW Methods. *Journal of Chemical Theory and Computation* **2018**, *14*, 5220–5228.
- (42) Loos, P.-F.; Scemama, A.; Duchemin, I.; Jacquemin, D.; Blase, X. Pros and Cons of the Bethe–Salpeter Formalism for Ground-State Energies. *The Journal of Physical Chemistry Letters* **2020**, *11*, 3536–3545.
- (43) Langreth, D.; Perdew, J. The gradient approximation to the exchange-correlation energy functional: A generalization that works. *Solid State Communications* **1979**, *31*, 567 – 571.
- (44) Gunnarsson, O.; Lundqvist, B. I. Exchange and correlation in atoms, molecules, and solids by the spin-density-functional formalism. *Phys. Rev. B* **1976**, *13*, 4274–4298.
- (45) Furche, F.; Van Voorhis, T. Fluctuation-dissipation theorem density-functional theory. *J. Chem. Phys.* **2005**, *122*, 164106.
- (46) Toulouse, J.; Gerber, I. C.; Jansen, G.; Savin, A.; Angyan, J. G. Adiabatic-Connection Fluctuation-Dissipation Density-Functional Theory Based on Range Separation. *Phys. Rev. Lett.* **2009**, *102*, 096404.
- (47) Toulouse, J.; Zhu, W.; Angyan, J. G.; Savin, A. Range-Separated Density-Functional Theory With the Random-Phase Approximation: Detailed Formalism and Illustrative Applications. *Phys. Rev. A* **2010**, *82*, 032502.

- (48) Angyan, J. G.; Liu, R.-F.; Toulouse, J.; Jansen, G. Correlation Energy Expressions from the Adiabatic-Connection Fluctuation Dissipation Theorem Approach. *J. Chem. Theory Comput.* **2011**, *7*, 3116–3130.
- (49) Olsen, T.; Thygesen, K. S. Static Correlation Beyond the Random Phase Approximation: Dissociating H₂ With the Bethe-Salpeter Equation and Time-Dependent GW. *J. Chem. Phys.* **2014**, *140*, 164116.
- (50) Maggio, E.; Kresse, G. Correlation Energy for the Homogeneous Electron Gas: Exact Bethe-Salpeter Solution and an Approximate Evaluation. *Phys. Rev. B* **2016**, *93*, 235113.
- (51) Holzer, C.; Gui, X.; Harding, M. E.; Kresse, G.; Helgaker, T.; Klopper, W. Bethe-Salpeter Correlation Energies of Atoms and Molecules. *J. Chem. Phys.* **2018**, *149*, 144106.
- (52) Li, J.; Drummond, N. D.; Schuck, P.; Olevano, V. Comparing Many-Body Approaches Against the Helium Atom Exact Solution. *SciPost Phys.* **2019**, *6*, 040.
- (53) Li, J.; Duchemin, I.; Blase, X.; Olevano, V. Ground-state correlation energy of beryllium dimer by the Bethe-Salpeter equation. *SciPost Phys.* **2020**, *8*, 20.
- (54) Salpeter, E. E.; Bethe, H. A. A Relativistic Equation for Bound-State Problems. *Phys. Rev.* **1951**, *84*, 1232.
- (55) Strinati, G. Application of the Green's Functions Method to the Study of the Optical Properties of Semiconductors. *Riv. Nuovo Cimento* **1988**, *11*, 1–86.
- (56) Blase, X.; Duchemin, I.; Jacquemin, D. The Bethe-Salpeter Equation in Chemistry: Relations with TD-DFT, Applications and Challenges. *Chem. Soc. Rev.* **2018**, *47*, 1022–1043.
- (57) Blase, X.; Duchemin, I.; Jacquemin, D.; Loos, P. F. The Bethe-Salpeter Formalism: From Physics to Chemistry. *J. Phys. Chem. Lett.* **2020**, *11*, 7371.
- (58) Hedin, L. On correlation effects in electron spectroscopies and the GW approximation. *J. Phys.: Cond. Mat.* **1999**, *11*, R489–R528.

- (59) Bruneval, F.; Vast, N.; Reining, L. Effect of self-consistency on quasiparticles in solids. *Phys. Rev. B* **2006**, *74*, 045102.
- (60) Gatti, M.; Bruneval, F.; Olevano, V.; Reining, L. Understanding Correlations in Vanadium Dioxide from First Principles. *Phys. Rev. Lett.* **2007**, *99*, 266402.
- (61) Vidal, J.; Trani, F.; Bruneval, F.; Marques, M. A. L.; Botti, S. Effects of Electronic and Lattice Polarization on the Band Structure of Delafossite Transparent Conductive Oxides. *Phys. Rev. Lett.* **2010**, *104*, 136401.
- (62) Rangel, T.; Kecik, D.; Trevisanutto, P. E.; Rignanese, G.-M.; Van Swygenhoven, H.; Olevano, V. Band structure of gold from many-body perturbation theory. *Phys. Rev. B* **2012**, *86*, 125125.
- (63) Tanwar, Akhilesh.; Fabiano, Eduardo.; Trevisanutto, Paolo Emilio.; Chiodo, Letizia.; Della Sala, Fabio, Accurate ionization potential of gold anionic clusters from density functional theory and many-body perturbation theory. *Eur. Phys. J. B* **2013**, *86*, 161.
- (64) Boulanger, P.; Jacquemin, D.; Duchemin, I.; Blase, X. Fast and Accurate Electronic Excitations in Cyanines with the Many-Body Bethe–Salpeter Approach. *J. Chem. Theory Comput.* **2014**, *10*, 1212–1218.
- (65) Knight, J. W.; Wang, X.; Gallandi, L.; Dolgounitcheva, O.; Ren, X.; Ortiz, J. V.; Rinke, P.; Körzdörfer, T.; Marom, N. Accurate Ionization Potentials and Electron Affinities of Acceptor Molecules III: A Benchmark of GW Methods. *J. Chem. Theory Comput.* **2016**, *12*, 615–626.
- (66) Li, J.; D’Avino, G.; Duchemin, I.; Beljonne, D.; Blase, X. Combining the Many-Body GW Formalism with Classical Polarizable Models: Insights on the Electronic Structure of Molecular Solids. *J. Phys. Chem. Lett.* **2016**, *7*, 2814–2820, PMID: 27388926.
- (67) Fujita, T.; Noguchi, Y. Development of the fragment-based COHSEX method for large and complex molecular systems. *Phys. Rev. B* **2018**, *98*, 205140.

- (68) Kang, W.; Hybertsen, M. S. Enhanced static approximation to the electron self-energy operator for efficient calculation of quasiparticle energies. *Phys. Rev. B* **2010**, *82*, 195108.
- (69) Hesselmann, A.; Gorling, A. Random-Phase Approximation Correlation Methods for Molecules and Solids. *Mol. Phys.* **2011**, *109*.
- (70) Colonna, N.; Hellgren, M.; de Gironcoli, S. Correlation Energy Within Exact-Exchange Adiabatic Connection Fluctuation-Dissipation Theory: Systematic Development and Simple Approximations. *Phys. Rev. B* **2014**, *90*, 125150.
- (71) Loos, P. F. QuAcK: a software for emerging quantum electronic structure methods. 2019; <https://github.com/pfloos/QuAcK>, <https://github.com/pfloos/QuAcK>.
- (72) Christiansen, O.; Koch, H.; Jørgensen, P. The second-order approximate coupled cluster singles and doubles model CC2. *Chem. Phys. Lett.* **1995**, *243*, 409 – 418.
- (73) Purvis, G. D.; Bartlett, R. J. A full coupled-cluster singles and doubles model: The inclusion of disconnected triples. *J. Chem. Phys.* **1982**, *76*, 1910–1918.
- (74) Christiansen, O.; Koch, H.; Jørgensen, P. Response functions in the CC3 iterative triple excitation model. *J. Chem. Phys.* **1995**, *103*, 7429–7441.
- (75) Huber, K. P.; Herzberg, G. *Molecular Spectra and Molecular Structure: IV. Constants of diatomic molecules*; van Nostrand Reinhold Company, 1979.
- (76) Krause, K.; Harding, M. E.; Klopper, W. Coupled-Cluster Reference Values For The Gw27 And Gw100 Test Sets For The Assessment Of Gw Methods. *Mol. Phys.* **2015**, *113*, 1952.